



NOVA

University of Newcastle Research Online

nova.newcastle.edu.au

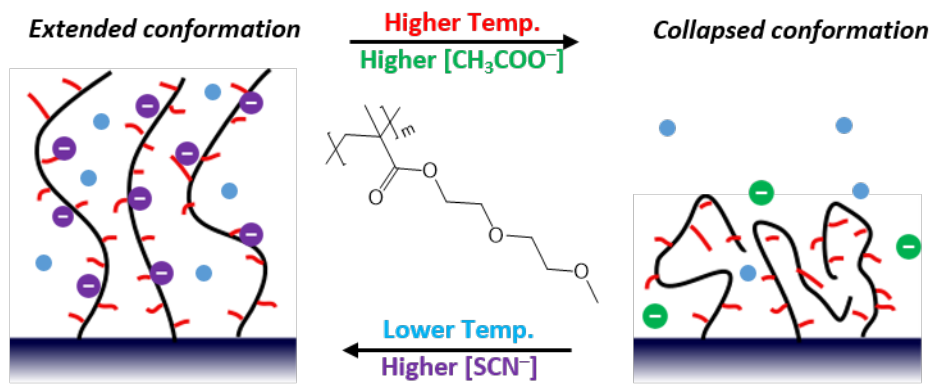
Murdoch, Timothy J.; Humphreys, Ben A.; Willott, Joshua D.; Prescott, Stuart W.; Nelson, Andrew; Webber, Grant B. & Wanless, Erica J. "Enhanced specific ion effects in ethylene glycol-based thermoresponsive polymer brushes" Published in *Journal of Colloid and Interface Science*, Vol. 490, p. 869-878, (2017).

Available from: <http://dx.doi.org/10.1016/j.jcis.2016.11.044>

© 2017. This manuscript version is made available under the CC-BY-NC-ND 4.0 license <http://creativecommons.org/licenses/by-nc-nd/4.0/>.

Accessed from: <http://hdl.handle.net/1959.13/1393372>

Graphical Abstract



Enhanced Specific Ion Effects in Ethylene Glycol-based Thermoresponsive Polymer Brushes

Timothy J. Murdoch,^a Ben A. Humphreys,^a Joshua D. Willott,^a Stuart W. Prescott,^b Andrew Nelson,^c
Grant B. Webber^a, Erica J. Wanless,^{a*}

^a Priority Research Centre for Advanced Particle Processing and Transport, University of Newcastle,
Callaghan, NSW 2308, Australia

timothy.murdoch@uon.edu.au

ben.humphreys@uon.edu.au

joshua.willott@uon.edu.au

grant.webber@newcastle.edu.au

erica.wanless@newcastle.edu.au

^b School of Chemical Engineering, UNSW Australia, UNSW Sydney, NSW 2052, Australia

s.prescott@unsw.edu.au

^c Australian Nuclear Science and Technology Organisation, Lucas Heights, NSW 2234, Australia

andrew.nelson@ansto.gov.au

*Corresponding author Erica J. Wanless, email: erica.wanless@newcastle.edu.au, phone: +61 2 4033
9355

Abstract

The thermoresponse of poly(di(ethyleneglycol) methyl ether methacrylate) (PMEO₂MA) brushes has been investigated in the presence of monovalent anions at either end of the Hofmeister series using ellipsometry, neutron reflectometry (NR) and colloid probe atomic force microscopy (AFM). NR measurements in deuterium oxide showed no evidence of vertical phase separation perpendicular to the grafting substrate with a gradual transition between a block-like, dense structure at 45 °C and an extended, dilute conformation at lower temperatures. All three techniques revealed a shift to a more collapsed state for a given temperature in kosmotropic potassium acetate solutions, while more swollen structures were observed in chaotropic potassium thiocyanate solutions. No difference was observed between 250 mM and 500 mM thiocyanate for a 540 Å brush studied by ellipsometry, while the lower molecular weight ~200 Å brushes used for NR and AFM measurements continued to respond with increasing salt concentration. The effect of thiocyanate on the temperature response was greatly enhanced relative to PNIPAM with the shift in temperature response at 250 mM being five times greater than a PNIPAM brush of similar thickness and grafting density.

Keywords (up to 10)

Thermoresponsive polymer

Responsive polymer

Polymer brush

Lower critical solution temperature

Poly oligo(ethylene glycol methacrylate)

Specific ion effect

Neutron reflectometry

Atomic force microscopy

Introduction¹

Thermoresponsive polymers that undergo significant conformational changes in response to small changes in temperature have a wide range of potential applications including controlled drug release and rheology modification.^{1,2} Poly(*N*-isopropylacrylamide) (PNIPAM) has been studied extensively owing to its limited response to environmental conditions (e.g. salt, pH, polymer concentration) and the fact that its lower critical solution temperature (LCST) occurs at a biologically relevant temperature (~32 °C in aqueous solution).² However, we have demonstrated anion specific conformations in PNIPAM brushes.³ In recent years, polymers formed from oligo ethylene glycol methacrylate (macro)monomers have emerged as viable alternatives to PNIPAM.⁴ The LCST of these poly oligo(ethylene glycol methacrylate) (POEGMA) polymers increases with the number (*n*) of hydrophilic ethylene glycol (EG) moieties in the side chain; statistical copolymerization using monomers with different values of *n* allows the LCST to be tuned between ~28 °C (poly(di(ethyleneglycol) methyl ether methacrylate, PMEO₂MA, Figure 1, *n* = 2) and 90 °C (*n* ~8.5).⁵ In addition, the PEG side chains impart biocompatibility,⁶ while PNIPAM is cytotoxic at ~37 °C.⁷

¹ Abbreviations

PNIPAM - poly(*N*-isopropylacrylamide)

LCST - lower critical solution temperature

POEGMA - poly oligo(ethylene glycol methacrylate)

PEG – poly(ethylene glycol)

PMEO₂MA - poly(di(ethyleneglycol) methyl ether methacrylate)

MW – molecular weight

NR – neutron reflectometry/reflectivity

AFM – atomic force microscopy/microscope

ARGET ATRP - activators continuously regenerated by electron transfer atom transfer radical polymerization

HMTETA – 1,1,4,7,10,10-hexamethyltriethylenetetramine

bipy - 2,2'-bipyridine

SMFS – single molecule force spectroscopy

POEGMA polymers show a comparable response with PNIPAM to polymer concentration and molecular weight (MW).⁴ Densely end-grafting these polymers to surfaces to form polymer brushes allows the switching of interfacial properties such as adhesion or lubrication and leads to applications as cell-culture substrates,⁸⁻¹¹ anti-fouling coatings^{12, 13} and controlled transport through membranes¹⁴ and chromatography materials.¹⁵

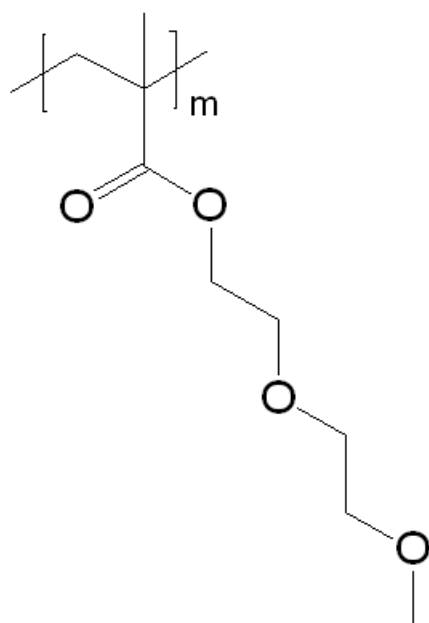


Figure 1. Structure of poly(di(ethyleneglycol)) methyl ether methacrylate (PMEO₂MA)

The thermoresponse of homo- and copolymer POEGMA brushes in aqueous solution has been characterized using ellipsometry,¹⁶ quartz crystal microbalance,¹⁷ contact angle,¹⁶⁻¹⁸ atomic force microscopy (AFM)¹⁹⁻²¹ and neutron reflectometry (NR) measurements.¹³ POEGMA brushes exhibit a smooth transition in bulk hydration and thickness over a broad temperature range (20 – 30 °C), as predicted by self-consistent field theory.^{17, 22, 23} Equilibrium contact angle measurements show that the surface of the brush collapses over a much narrower temperature range, giving indirect evidence of a first-order phase transition.¹⁷ However, no direct evidence of vertical phase separation was seen in the NR measurements of Gao et al.¹³ AFM adhesion measurements show that POEGMA brushes are less adhesive than PNIPAM brushes.^{19, 21} While highly reversible, Kessel et al. report time

dependent adhesion at temperatures greater than the LCST.²⁰ This parallels the observation that the hydrophilic PEG side chains on free POEGMA chains in solution rearrange themselves to maximize contact with the solvent at temperatures above the LCST.²⁴

Specific ion effects are any phenomena which depend on the identity of the ions present in solution and not simply their concentration.²⁵ First identified by Franz Hofmeister in 1888 for work on protein stability,²⁶ they have since been observed to affect a wide range of systems including responsive polymer gels²⁷ and brushes,^{3, 28-31} bubble coalescence³² and the stability of colloidal particles.³³ Specific ion effects have been widely characterized for free PNIPAM³⁴ and POEGMA³⁵ chains in solution, and are found to depend on the location of the ions in the Hofmeister series. In particular, salts containing hard, strongly hydrated anions lower the LCST while those containing soft, poorly hydrated anions will raise the LCST at low-to-intermediate concentrations. The specific ion responses of POEGMA variants are expected to be more significant than that of PNIPAM as a result of the extensive hydration of the side chains.³⁵ We have previously reported that the presence of salt translates the swollen state of PNIPAM brushes to lower or higher temperatures in the presence of acetate and thiocyanate anions respectively.^{3, 36} However, the initial swelling of the brush was found to be less temperature sensitive in the presence of thiocyanate anions. Several studies of POEGMA copolymers have demonstrated that physiological buffer solutions have a salting out effect relative to pure water.^{13, 37, 38} While biologically relevant, the choice of a single buffer does not allow the specific ion response to be systematically investigated.

Herein we present an investigation of the influence of specific ions from the two extremes of the Hofmeister series on the thermoresponse of homopolymer PMEO₂MA brushes using complementary ellipsometry, NR and AFM force measurements. The presence of the anions results in a greater shift in the temperature response compared to the more widely studied PNIPAM system. In contrast to PNIPAM brushes,³ the NR density profiles reveal no evidence of vertical phase separation during the temperature induced collapse.

Materials and Methods

Materials

Native oxide silicon wafers (100 mm diameter, 10 mm thick) were purchased from El-Cat Inc. (USA) for specular neutron reflectometry (NR) experiments. Native oxide silicon wafers for ellipsometry and atomic force microscopy (AFM) experiments were purchased from Silicon Valley Microelectronics (USA). Potassium hydroxide (Chem-Supply Pty Ltd, AR grade) was used during surface preparation steps. Surface functionalization reagents (3-aminopropyl)triethoxysilane (APTES, >99%) and 2-bromoisobutyryl bromide (BIBB, >99%) were purchased from Sigma-Aldrich and used as received. The tetrahydrofuran (THF, Honeywell Burdick and Jackson, >99%) and triethylamine (Eth₃N, Sigma-Aldrich, 99%) were dried over 4 Å molecular sieves (ACROS Organics) before use. Polymerization reagents including the catalyst copper(II) bromide (CuBr₂, 99.999%), ligands 2,2'-bipyridine (bipy, ≥99%) and 1,1,4,7,10,10-hexamethyltriethylenetetramine (HMTETA, 97%), and reducing agent (+)-sodium L-ascorbate (>98%) were purchased from Sigma Aldrich and used as received. 2-(2-methoxyethoxy)ethyl methacrylate (MEO₂MA, Sigma-Aldrich, 95%) was gravity fed through a 10 cm long, 2 cm diameter alumina column (activated, basic) to remove the 100 ppm hydroquinone monomethyl ether and 300 ppm butylated hydroxytoluene inhibitors immediately prior to use. Aqueous solutions of potassium acetate (KCH₃COO, Alfa Aesar, >99%) and potassium thiocyanate (KSCN, Alfa Aesar, >98%) were prepared and used. The pH of the electrolyte solutions was controlled at pH 5.5 ± 0.1, with adjustment made by the addition of potassium hydroxide (Chem Supply Pty Ltd, >99%) and acetic acid (Ajax Finechem Pty Ltd, 100%, for acetate solutions) or nitric acid (RCI Labscan Ltd, AR grade, for thiocyanate solutions). Appropriate corrections for pD were used during NR experiments. Ethanol (Ajax Finechem Pty Ltd, absolute) was distilled before use, methanol (Sigma Aldrich, anhydrous, 99.8%) was used as received and MilliQ™ water (Merck Millipore, 18.2 MΩ-cm at 25 °C) was used throughout. Specular neutron reflectometry measurements were

performed in pure deuterium oxide (D_2O) with all salt solutions prepared using pre-filtered (0.45 μm disk filters) D_2O .

PMEO₂MA Brush Synthesis

Silicon wafers for ellipsometry and AFM were cleaned and initiator-functionalized following our established protocol, with the method up-scaled for the 100 mm NR silicon wafers.³ The 'grafted from' activators continuously regenerated by electron transfer atom transfer radical polymerization (ARGET ATRP) method³⁹ was used to synthesize PMEO₂MA brushes from the surface bound bromine initiator moieties. Two separate ARGET ATRP recipes were utilized for synthesis depending on desired brush thickness. A combination of MEO₂MA/CuBr₂/bipy/sodium ascorbate in the molar ratios of 2500/1/10/10 was used with a solvent mixture of methanol/H₂O at 4:1 v/v to prepare the thin brushes for NR and colloid probe AFM experiments. To prepare the thicker brush required for in situ ellipsometry experiments MEO₂MA/CuBr₂/HMTETA/sodium ascorbate in the molar ratios of 2500/1/10/10 was used with methanol as the solvent to increase the polymerization rate (see Figure S1 and accompanying discussion). The ratio of solvent mixture to MEO₂MA monomer was 1:1 v/v. For a more detailed brush synthesis protocol see the Supporting Material.

Table 1 summarizes the different brushes synthesized for this study with dry thickness determined by ellipsometry and single molecule force spectroscopy (SMFS) respectively as outlined below and in the Supporting Material. The brush thickness used for each technique was chosen to optimize the quality of the data; ellipsometry required a thicker brush to get reliable changes in measured Δ and ψ values, while resolution effects in neutron reflectometry mean that the upper limit of the swollen brush thickness should be 1000 Å or less. Relatively thin brushes were synthesized for the SMFS study to ensure all adhesion events were within the translation range of the AFM scanner. Colloid probe AFM measurements are sensitive to a smaller population of higher MW chains with a lower effective grafting density at the periphery of the brush and, consequently, it is difficult to separate the contribution of MW and the lower local concentration of polymer (both shown to affect the specific ion response of free chains in solution). Such a distribution of chains becomes more

probable in thicker brushes (with increasing synthesis time), so a relatively thinner brush was also used for colloid probe AFM experiments.

Table 1. Details PMEO₂MA brush samples studied by each technique used.

Experiment	Ligand and Solvent	Dry brush thickness by ellipsometry (Å)	Grafting density by SMFS (nm ⁻²)
Ellipsometry	HMTETA	540 ± 30	0.07 ± 0.02
AFM (SMFS)	MeOH	250 ± 20	
Neutron reflectometry	Bipy MeOH:H ₂ O (4:1)	140 ± 10	0.05 ± 0.01
AFM (colloid probe)		215 ± 10	
AFM (SMFS)		148 ± 10	

Ellipsometry

Ellipsometry experiments were conducted on a Nanofilm EP3 single wavelength (532 nm green laser) imaging ellipsometer controlled by EP3View software. WVASE32 software was used to model the ellipsometric parameters (Δ and ψ). The experimental methodology of dry and in situ ellipsometry measurements was identical to our earlier study.³⁶ All brushes are referred to by their dry thickness as measured by ellipsometry (shown in Table 1), as all brushes were characterized using this technique. In situ ellipsometry measurements were performed on a 540 ± 30 Å dry thickness PMEO₂MA brush. The following sigmoidal function was used to fit the thickness as a function of temperature T :

$$y = A + \frac{B}{1 + \exp(k(T_0 - T))} \quad (1)$$

where A (Å) and B (Å) are constants related to the thickness at low and high temperature respectively, k (°C⁻¹) is a constant related to the steepness of the transition and T_0 is the temperature at which the thickness has increased by 50%. T_0 has been used as the reference swelling state for the swollen-collapse transition. As with our earlier study, in situ measurements were measured from high to low temperature to prevent bubble formation within the cell.³⁶

X-ray Reflectometry

A Panalytical X'Pert Pro X-ray reflectometer (with CuK α radiation $\lambda = 1.541 \text{ \AA}$) was used to characterize the dry brush ($143 \pm 2 \text{ \AA}$) prepared on the 100 mm silicon wafer prior to neutron reflectometry. Specular reflectometry measurements were made as a function of the scattering vector, $Q = \frac{4\pi}{\lambda} \sin \theta$, where λ is the wavelength and θ is the angle of incidence. Data were analyzed using the MOTOFIT package.⁴⁰

Neutron Reflectometry

NR measurements were carried out on the *Platypus* time-of-flight reflectometer at the OPAL 20 MW reactor (Australian Nuclear Science and Technology Organisation, Sydney, Australia).⁴¹ Specular reflectivity measurements were performed at angles of incidence of 0.8° and 3.8° (0.6° and 2.8° in air) furnishing reflection data over the Q range of 0.009 to 0.31 \AA^{-1} (0.007 to 0.24 \AA^{-1} in air) at a constant dQ/Q resolution of 8%.⁴¹ Experiments were carried out in a standard solid-liquid fluid cell with the temperature set by temperature control jackets. Temperature was changed from high to low; matching the ellipsometry measurements. Initial measurements at an angle of incidence of 0.8° revealed that the sample was thermally equilibrated within ~ 1 min of the sample reaching the target temperature. Sample temperature was monitored via a thermocouple attached to the silicon block. Our previous study confirmed through conductivity measurements that the volumes used in solution changes were adequate for complete solvent exchange.⁴²

Analysis of Neutron Reflection Data

Neutron reflectometry is sensitive to changes in scattering length density (SLD, ρ_N) perpendicular to the substrate. Data were analyzed using a custom model implemented in MOTOFIT.^{3, 40} The model consisted of a native SiO₂ layer followed by a small number of layers (≤ 3) of constant volume fraction that represents the interior (i.e. closest to the substrate) of the brush. The interfaces between these layers are smoothed with Gaussian roughness. If required, an analytical Gaussian decay was used to model the dilute, tail region of the brush:⁴³

$$\phi(z) = \phi_0 \exp\left(-\frac{(z-z_0)^2}{H^2}\right) \quad (2)$$

where $\phi(z)$ is the volume fraction at distance z (Å), z_0 (Å) is the distance at the start of the tail region of the brush, H (Å) is the characteristic height of the exterior tail region, ϕ_0 is the initial volume fraction at the boundary between the interior and exterior tail regions. To calculate the reflectivity, the tail region was discretized into 50 layers of constant volume fraction with a small Gaussian roughness term equal to a third of the layer thickness connecting each layer. To give the profile a finite thickness, the tail was truncated at $\phi(z) = 0.005$. The SLD of each brush layer was then calculated from the volume fraction weighted sum of each component:

$$\rho_N(z) = \phi(z)\rho_{N,PMEO_2MA} + (1 - \phi(z))\rho_{N,Solv} \quad (3)$$

where $\rho_{N,Solv}$ is the SLD of the solvent. The reflectivity was then calculated using the Abeles matrix method.⁴⁰

Initial fitting showed that increasing the SLD of the native SiO₂ layer greatly improved the quality of the fits at high temperatures. Co-refinement of the NR measurements on the brush in air and at the highest temperature for each salt condition showed 13.5 % solvent penetration into the SiO₂ layer; this value was applied to all subsequent fits (see Figure S2). At high temperatures, only a single layer of collapsed polymer was required to fit the data, increasing up to three layers as the brush began to swell at lower temperatures. A combination of a single interior layer and a Gaussian tail was only required for the most swollen conditions. Fitting parameters for each condition are summarized in Tables S1-4.

The feasibility of each fit was checked by calculating the effective dry thickness, $\delta = \int_0^\infty \phi(z)dz$, as the covalent binding of the polymer to the surface means that δ should be constant throughout all dry and wet measurements. The constant nature of δ between measurements in air and salt solutions allowed the polymer SLD ($0.94 \times 10^{-6} \text{ \AA}^{-2}$) and corresponding bulk density (1.26 g cm^{-3}) to be determined using the co-refinement method of Murdoch et al³ and is within error of the values determined by Laloyaux et al. using XRR.¹⁷ A Lagrange multiplier was used to penalize fits with unreasonable adsorbed amounts during the minimization process.³

The average brush thickness, L_{1st} , was determined by twice the normalized first moment of the volume fraction profile:

$$L_{1st} = 2 \frac{\int_0^{\infty} z\phi(z)dz}{\delta_{dry}} \quad (4)$$

A factor of 2 is used in Equation 4 as this corresponds to the thickness of a step-density profile with the same normalized first moment.⁴⁴

Atomic Force Microscopy

Normal force measurements were performed using a Bruker MultiMode 8 AFM with a vertical engage EV scanner in contact mode equipped with a closed fluid cell (Bruker, USA). The entire AFM was housed in an incubator allowing accurate temperature control (within 0.5 °C) between 10 and 40 °C. The sample was equilibrated overnight in pure water prior to initial measurements. Each condition was measured from 10 to 40 °C in order to minimize potential evaporation through the fluid cell spring clip and reduce the time spent at high temperature for the AFM electronics. A minimum of 15 min was allowed for equilibration once the cell temperature had been reached. Description of the cantilevers used in this study, the preparation of the silica colloid probe and cleaning protocols are provided in the Supporting Material. Single molecule force spectroscopy (SMFS) experiments were performed on PMEO₂MA brushes (from each polymerization recipe) of dry thicknesses 250 Å and 148 Å, while the colloid probe measurements were performed on a PMEO₂MA brush of dry thickness 215 Å (see Table 1). Details of the SMFS and colloid probe measurements are provided in the Supporting Material.

Results and Discussion

Thermoresponse in Pure Water

Self-consistent field theories of polymer brushes predict a broadening of the swollen-collapsed transition of brushes with decreasing solvent quality;⁴⁵ thermoresponsive polymers with an LCST type transition are therefore expected to exhibit a collapse over a wider temperature range than the

ungrafted chain transition as temperature is increased.²³ Figure 2 demonstrates that a broad collapse is indeed evident in the response of a 540 Å brush measured by ellipsometry, with the brush responding over a temperature range of 30 °C in water. The reported temperature range is approximately double that of a PNIPAM brush of comparable grafting density and dry thickness.³⁶ While the LCST transition of ungrafted chains measured by transmittance is sharp for both PNIPAM and PMEO₂MA,⁴ POEGMA polymers have been shown to continue to dehydrate at temperatures above the LCST;²⁴ continued dehydration of the sidechains likely contributes to the broadening of the collapse transition. A sigmoidal fit to the PMEO₂MA data in water gives a transition temperature of 21.2 ± 0.2 °C which is close to the value of 22.2 °C reported by Laloyaux et al. for a 920 Å PMEO₂MA brush, who report a transition width of 20 – 30 °C.¹⁷

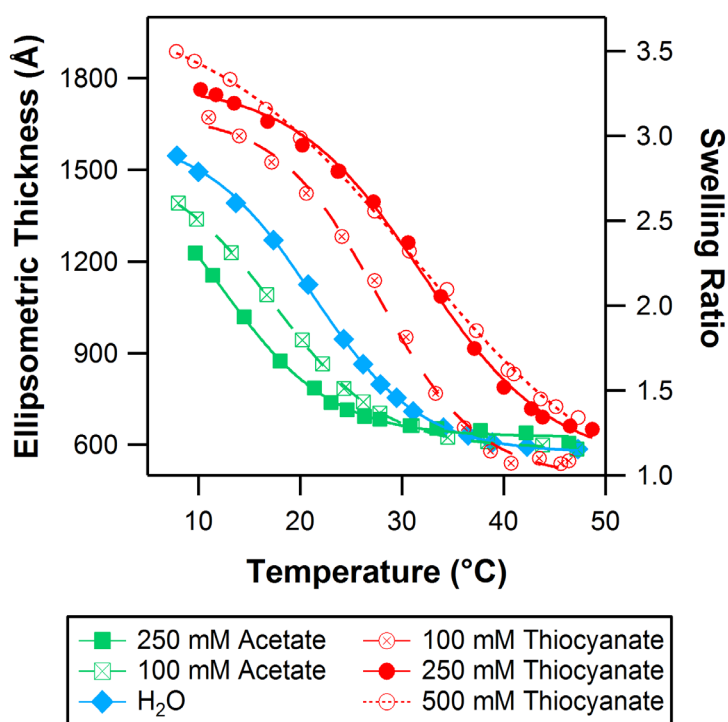


Figure 2. Ellipsometric thickness of a 540 ± 30 Å PMEO₂MA brush as a function of temperature for solutions of differing salt concentration and identity. Lines are sigmoidal fits to the data (Equation 1). The swelling ratio is the wet thickness at each condition normalized by the dry brush thickness.

Neutron reflectivity data for the temperature response of a PMEO₂MA brush in D₂O, and associated volume fraction profiles, are presented in Figure 3. Reflectivity data in Figure 3a has been presented as RQ^4 , which highlights features arising from deviation to the Q^{-4} decay predicted by Fresnel's law for a bare interface. At high temperature (≥ 30 °C) the reflectivity is dominated by strong Kiessig fringes, indicating a well-defined, block-like, collapsed, profile. The overestimation of the depth of minima around 0.08 \AA^{-1} by the model reflectivity data likely arises from a degree of lateral inhomogeneity in the polymer film.³ As the temperature is decreased, Kiessig fringes are damped and the minima shift to lower values of Q as the brush swells to form an extended, diffuse interface. The model for the swollen brush data requires a thin, dense layer of polymer near the substrate, and is associated with the oscillation in the reflectivity at $Q \sim 0.05 \text{ \AA}^{-1}$. These thin layers are often present in model volume fraction profiles of brushes in NR experiments and may result from polymer adsorption to the substrate^{3, 46-49} or bimodal molecular weight distributions⁵⁰ that aren't accounted for in most polymer brush theories. The volume fraction profiles, Figure 3b, show the swelling response of the PMEO₂MA brush, where the single, dense slab conformation at low high temperature transitions to an inner slab with extended, well-hydrated tail at low temperatures. Consistent with Gao et al.¹³ and in contrast to PNIPAM brushes investigated by NR,^{3, 51, 52} there is no evidence of vertical phase separation of the brush; that is, no distinct separation into a bilayer profile is observed for temperatures measured. The grafting density of the brush²² and the dynamic rearrangement of the ethylene glycol side chains for temperatures above the LCST²⁴ may also contribute to the smooth transition between a block-like and extended conformation.

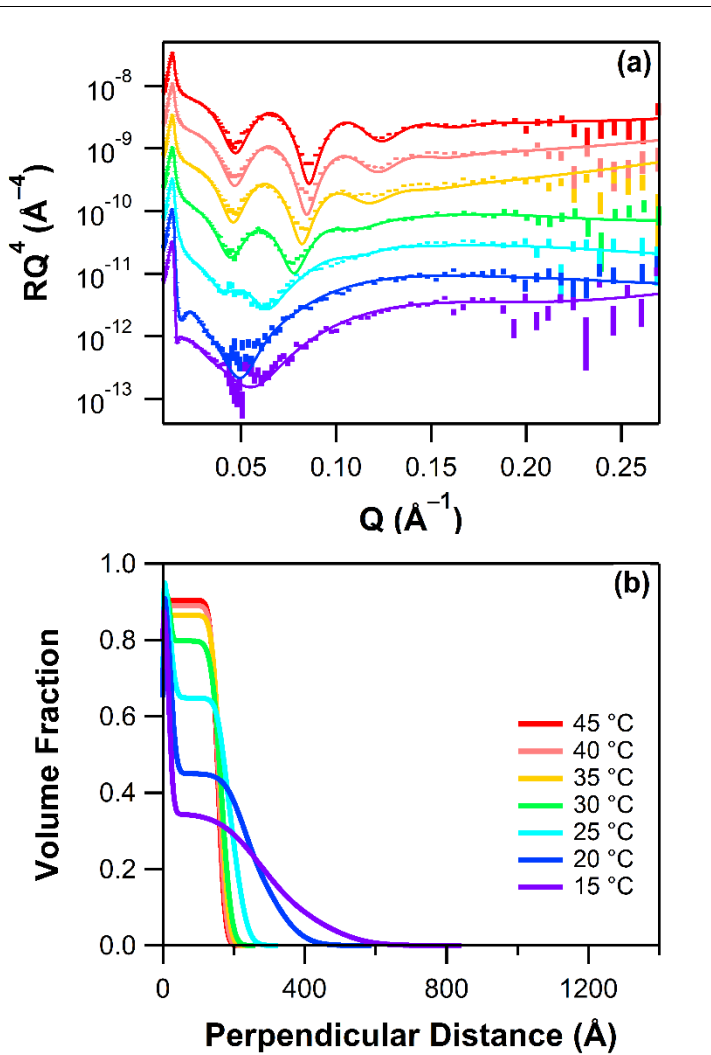


Figure 3. (a) Neutron reflectivity data and (b) corresponding volume fraction profiles for a $140 \pm 10 \text{ \AA}$ PMEO₂MA brush in D₂O showing the transition from a dense, uniform block of mostly dehydrated polymer at high temperatures to an extended, solvated polymer brush as the temperature is reduced. Data in (a) is offset for clarity, with the data for 45 °C plotted using measured values.

Figure 4 shows representative AFM force versus apparent separation curves for a colloid probe interacting with a $215 \pm 10 \text{ \AA}$ PMEO₂MA brush in water as a function of temperature. The approach curves in Figure 4a consist of a long-range attraction, followed by a repulsive, compressive region that is highlighted in the log-linear inset plot. The linear nature of this region demonstrates that the increase in force during the compression of the brush is approximately exponential as predicted by

the Alexander–de Gennes and Milner–Witten Cates theories for polymer brushes in a good solvent.³¹ Attraction on approach has been seen previously for neutral polymer brushes and is associated with bridging interactions between the colloid probe and extended chains.^{3, 53} Upon retraction, Figure 4b, adhesive interactions are observed. As the probe penetrates and compresses the brush during the approach phase individual chains within the brush interact directly with the colloid probe. These chains are then stretched over a significant distance upon retraction of the probe before detaching. The shape of the curve represents the continuous detachment of multiple-chains rather than single pull-off events.²⁰ Whilst the silica probe will be negatively charged at the solution pH used it is unlikely this interaction is electrostatic in origin as the PMEO₂MA brush is uncharged. Oligo(ethylene glycol) molecules are well-known to exhibit strong hydrogen bonding,⁵⁴ and it is likely there is a hydrogen-bond type interaction between the ethylene glycol side chain of the MEO₂MA residues and the silica probe. In addition, adhesion will occur due to dispersive van der Waals interactions as the brush and probe are forced into contact. The observed trend in the magnitude of the adhesion is consistent with a transition from an extended hydrophilic brush to a simultaneous detachment of multiple chains promoted by preferred polymer-polymer interactions with increasing temperature.^{20,}

⁵⁵ This is consistent with Yu et al., who observed an increase in the adhesion between a PNIPAM brush and a gold colloid as the brush was progressively more collapsed.⁵⁵

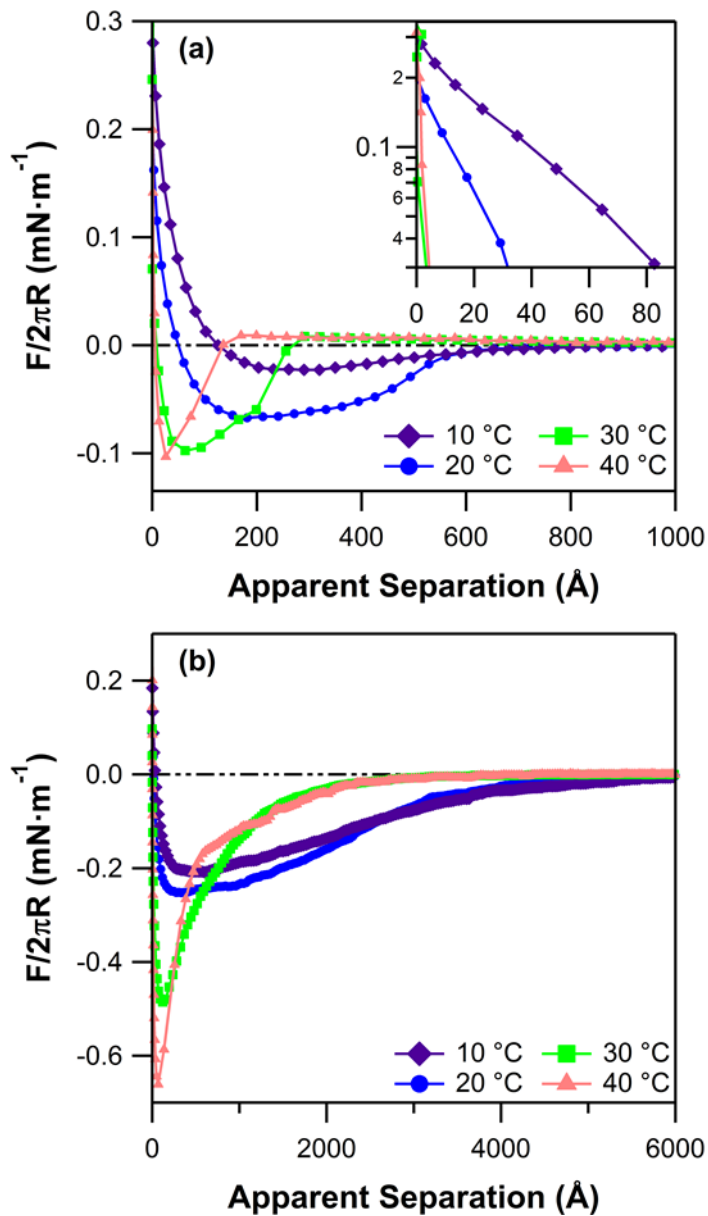


Figure 4. Force versus apparent separation measured in water for the interaction of a $15\ \mu\text{m}$ colloid probe and a $215 \pm 10\ \text{\AA}$ PMEO₂MA brush during (a) approach and (b) retraction. Inset to (a) shows the approach data at close separation on a log-linear scale.

The techniques used above were measured in a single ramp with temperature either increasing or decreasing due to instrumental and time considerations (as explained in the Materials and Methods section). Recent work by Varma et al., has demonstrated that swelling hysteresis is not observed for

thermoresponsive PNIPAM brushes with dry thickness less than 150 Å.⁵⁶ PNIPAM chains free in solution show significantly larger hysteresis than POEGMA based polymers.⁴ Furthermore, no hysteresis was observed for a 780 Å dry thickness PMEO₂MA brush by Zhuang et al.¹⁶ Therefore, no significant swelling hysteresis is expected for the brushes reported in this article.

Thermoresponse in Aqueous Salt Solutions

The thermoresponse of PNIPAM^{3, 34, 36} and POEGMA³⁵ variants in aqueous salt solutions is dependent on the ionic strength and the location of the ions in the Hofmeister series. Changing the anion tends to produce a larger specific ion response, in part due to a wider range of polarizable volumes of anions.²⁵ We have probed the specific ion response of POEGMA brushes using potassium salts with anions at either end of the Hofmeister series; strongly hydrated acetate ions (kosmotropic) and weakly hydrated thiocyanate (chaotropic). The LCST of free POEGMA and PNIPAM in solution is lowered in the presence of kosmotropic salts as they can polarize H-bonded water and make hydration of the hydrophobic backbone of the polymer unfavourable.³⁴ Chaotropic thiocyanate anions, which have an affinity for hydrophobic interfaces,^{25, 57, 58} can bind directly to the polymer chain, increasing the charge. The higher charge on the chains provides electrosteric stabilization and raises the LCST. Importantly, binding is a saturation phenomenon^{34, 59} and sufficiently high concentrations of thiocyanate will lower the LCST of the polymer.

Ellipsometry data in Figure 2 shows the swelling of a 540 ± 30 Å brush in response to temperature, ionic strength, and anion identity. Consistent with our previous studies of PNIPAM brushes,^{3, 36} the principal impact of the addition of salt is a translation of the overall temperature response along the temperature axis. Increasing acetate concentration shifted the response to lower temperatures while increasing thiocyanate concentration up to 250 mM shifts the response to higher temperatures. A further increase in the concentration of thiocyanate to 500 mM did not significantly shift the swelling response, suggesting that the direct binding mechanism was saturated. Higher concentrations of potassium acetate were not studied as condensation on cell windows precludes

access to the lower temperatures required to observe any further movement of the thermoresponse.

Figure 5 demonstrates the effect of temperature and salt concentration and identity on the conformation of a $140 \pm 10 \text{ \AA}$ polymer brush measured by NR. Corresponding reflectivity data may be found in Figure S3. Similar to the response in pure D_2O (Figure 3), at high temperatures block-like conformations are formed with a relatively small increase in brush hydration with decreasing temperatures. At low enough temperature the brush starts to swell significantly through the formation of a single dilute swollen phase. Further decreasing the temperature results in the gradual extension of this swollen phase. This behavior is consistent with the change in average height (Equation 4) with decreasing temperature as shown in Figure 6, i.e. a region of constant thickness at high temperature and a monotonic increase in thickness with decreasing temperatures at lower temperatures. The volume fraction profiles and average thicknesses show that extended, decaying profiles are more prevalent across the temperature ranges studied with increasing thiocyanate concentration up to at least 500 mM. Conversely, in 250 mM acetate the brush swells to a lesser extent, even at the lowest temperature measured. Again, condensation at low temperature and an expected shift in the LCST to lower temperatures in D_2O solutions, $\sim 1.4 \text{ }^\circ\text{C}$ reported previously for ungrafted POEGMA copolymer in salt-free D_2O ,²⁴ limit the accessible concentration range for acetate solutions.

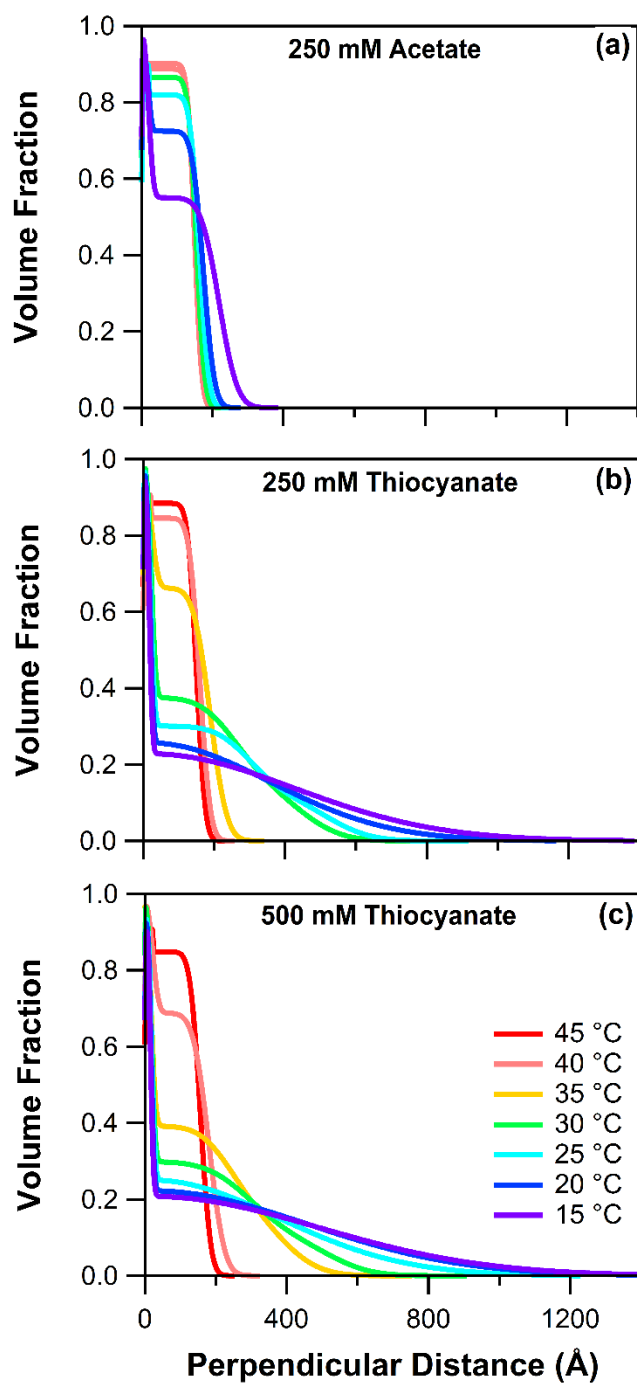


Figure 5. Extracted volume fraction profiles as a function of temperature brush of a 140 ± 10 Å PMEO₂MA immersed in (a) 250 mM potassium acetate, (b) 250 mM thiocyanate, and (c) 500 mM thiocyanate D₂O solutions. The extent of the diffuse tail of the brush is seen to be strongly influenced by the identity of the anion.

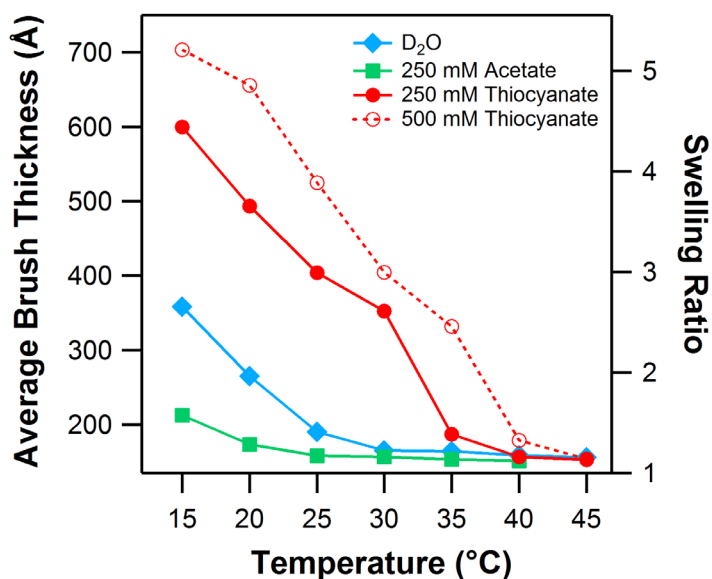


Figure 6. Average brush thickness as a function of solution temperature for a 140 Å PMEO₂MA brush immersed in pure D₂O and salt solutions of varying anion identity and concentration. Thicknesses are extracted from the volume fraction profiles (Figure 5) determined by neutron reflectometry. The swelling ratio is the wet thickness at each condition normalized by the dry brush thickness.

Approach data for the AFM colloid probe salt study is shown in Figure 7. The NR and ellipsometry data show that the PMEO₂MA brushes are collapsed in 250 mM potassium acetate, relative to water, for a given temperature below the swelling transition. The inset data in Figure 7a and 7b, corresponding to 10 °C and 20 °C, appear to contradict this as they show a larger range of compression in acetate. However, the absolute separation between the colloid probe and underlying silica surface is not known, with zero corresponding to the separation at which constant compliance is reached; hence direct comparison is difficult. A better comparison is to compare the range over which attractive bridging interactions are observed. Consistent with the volume fraction profiles shown in Figure 5, force curves in salt-free water display a longer range attraction than in 250 mM acetate which suggests that there is a longer, dilute tail region that can interact with the probe before the bulk of the brush is reached. At 10 °C, the approach curves are purely repulsive in the

presence of thiocyanate at 250 and 500 mM suggesting a stronger degree of hydration of the brush reducing direct contact between polymer chains and the probe.²⁰ At 20 °C only the 500 mM thiocyanate approach is purely repulsive, with a weak, long range attraction observed in 250 mM thiocyanate. Further increase in temperature to 30 °C results in a reduction in the range of bridging for all conditions. NR data for a brush of similar thickness (Figures 3 and 5) show that the brush is in a collapsed, block-like conformation that contains ~10 % water at 40 °C for all solutions. A block-like structure is consistent with short range of compression observed in the AFM data at 40° C (Figure 7d) in all conditions. The retention of short-range bridging interactions suggests the presence of a small population of dilute chains that aren't detected by NR measurements.

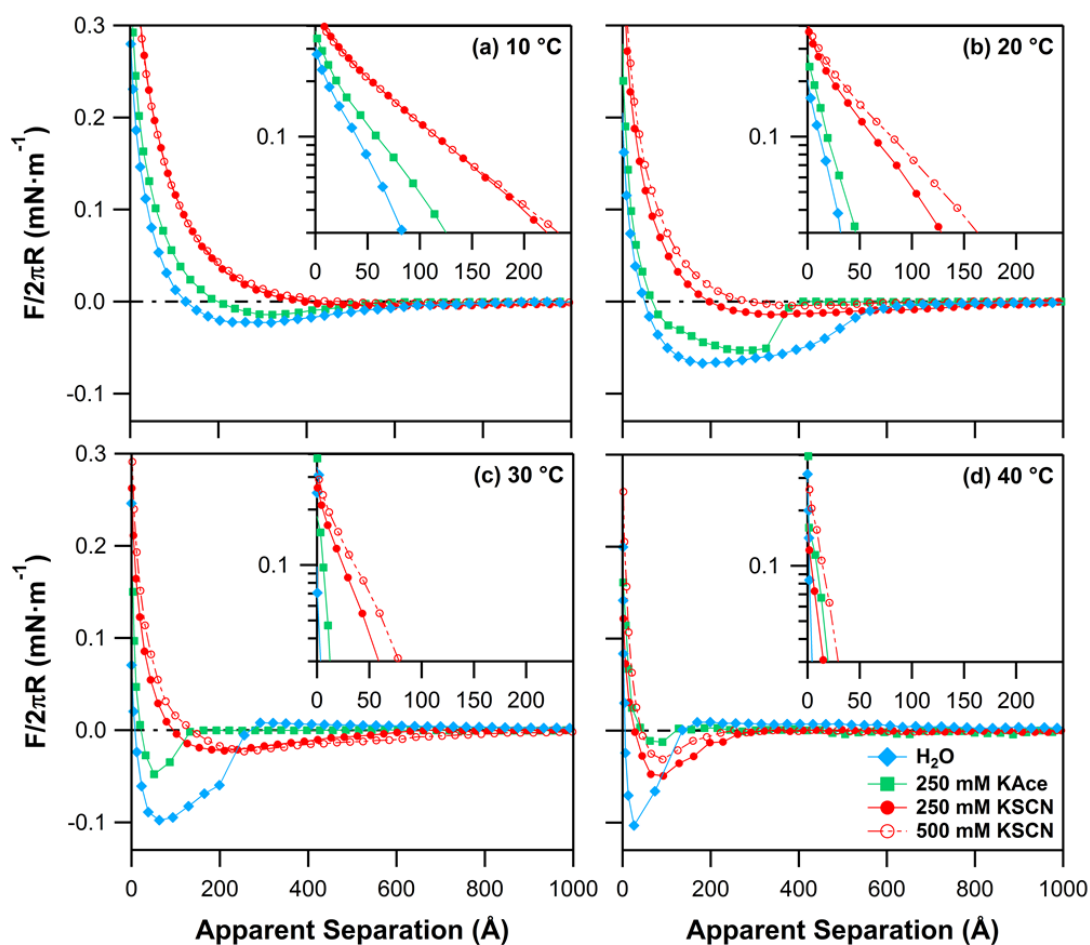


Figure 7. Force versus apparent separation curves for the approach of a silica colloid probe toward a $215 \pm 10 \text{ Å}$ PMEO₂MA brush in pure H₂O, 250 mM potassium acetate, 250 mM potassium thiocyanate and 500 mM potassium thiocyanate. Inset plots (log-linear) highlight the repulsive region of the approach curves. The strength and range of the attractive interaction are indicative of the presence of a diffuse tail of polymer extending into the solution, as shown in the volume fraction profiles in Figure 5.

The complementary AFM retraction data to Figure 7 are displayed in Figure S4. These data confirm the anion-specific thermoresponsive behavior of the PMEO₂MA brush observed in the approach data. At 10 °C, Figure S4a, the data in water and the three salt solutions is qualitatively similar; an adhesion upon retraction that extends to over 4000 Å apparent separation. In each case the range of adhesion is far greater than the corresponding interaction upon approach and is indicative of a

swollen brush. As the temperature is increased to 20 °C the retraction data changes markedly in 250 mM acetate only (Figure S4b). Here the range of the interaction is significantly decreased, and the return to the zero-force baseline is much sharper. Since the brush is collapsed at 20 °C in 250 mM acetate, see Figures 2 and 6, there is reduced interaction between the polymer chains and the colloid during contact. As the temperature is increased further the AFM retraction data supports the ellipsometry, NR and AFM approach data; at 30 °C the brush is collapsed in pure water (Figure S4c), but only collapses in the presence of thiocyanate anions at 40 °C (Figure S4d). Across this range there is little change in the approach data in 250 mM acetate, indicating the brush may be fully collapsed. Interestingly at 40 °C, where the brush is collapsed in all solutions, the range of adhesion upon retraction is similar in all cases but the magnitude is much greater in salt-free water. This indicates the presence of salt is modulating the interaction between the collapsed brush and the colloid probe.

For these thermoresponsive brushes, defining an LCST is unhelpful given the breadth of the temperature response. Instead, we can assess the influence of salt on the thermoresponse of PMEO₂MA brushes by comparing the shift in temperature to achieve the same swelling state. The ellipsometry and NR data in Figures 1 and 6 are both measures of average brush thickness.¹⁶ Comparing the data in these Figures, there is a clear trade-off between the complexity of the analysis offered by NR (e.g. volume fraction profiles in Figures 3 and 5) and the density of data points. The greater temperature range and resolution readily afforded by ellipsometry (NR experiment time is scarce) allows the half-height of a sigmoidal fit to the data calculated from Equation 1 to be used as a reference swelling state, with the temperature shift relative to H₂O shown in Figure 8. This fitting indicates the saturation of the thiocyanate response may have occurred in the ellipsometry experiment, with the maximum temperature shift in thiocyanate being ~ 10 °C. To estimate the temperature shift for the NR data a brush thickness of 215 Å was chosen as a reference point, corresponding to the average brush thickness in 250 mM acetate at 15 °C. This thickness value was chosen as it is achieved in all conditions and represents a marked increase in

swelling ratio relative to collapsed state. This estimate shows that the response in potassium acetate is similar for the brushes used for both ellipsometry and NR measurements and is of similar magnitude to free POEGMA chains in solution of sodium acetate.³⁵

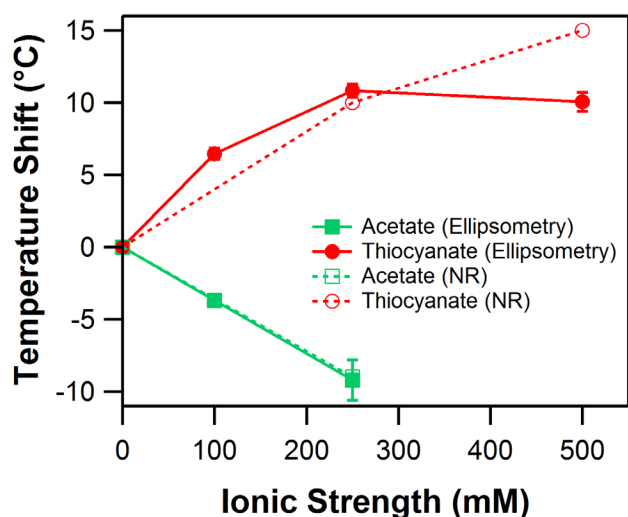


Figure 8. Temperature shift of the reference swelling state of PMEO₂MA brushes immersed in solutions of differing salt concentration and identity, relative to salt-free water. Solid lines correspond to a $540 \pm 30 \text{ \AA}$ brush measured by ellipsometry with the half-width of a sigmoidal fit used as the reference point. Dotted lines correspond to a $140 \pm 10 \text{ \AA}$ brush measured by NR, with a swollen brush thickness of $215 \pm 10 \text{ \AA}$ used as the reference state.

In contrast to the ellipsometry data, the NR response in potassium thiocyanate does not saturate in the concentration range studied. While a reference swelling state is difficult to determine, the AFM colloid probe measurements also show a continued shift in response up to at least 500 mM. Given the similar grafting densities (Table 1) of the brushes from the two synthetic conditions, there may be a contribution of polymer MW to the interaction with thiocyanate; recall that due to instrumental limitations the brush measured by ellipsometry was thicker than that used in NR experiments. A broader range of salt concentration and brush thickness would need to be investigated to further

elucidate the relationship between chaotrope saturation and MW in polymer brushes. Spectroscopic ellipsometry measurements would be capable of reliably measuring changes in solvated brushes over a wide range of brush thickness. Moreover, the MW dependency on the salt response of neutral thermoresponsive polymer has been studied previously by Zhang et al.⁶⁰ for a range of MW for free PNIPAM chains. Both the salt concentration dependence and magnitude of the peak increase in LCST in the presence of chaotropes were found to increase with decreasing MW. They proposed that increased intrachain interactions with increasing MW reduce the number of potential binding sites for chaotropes.⁶⁰ The saturation of the thiocyanate response shown in Figure 8 for the higher MW is therefore consistent with the behavior of free PNIPAM chains in solution.

We have previously reported a shift in temperature response of a 566 ± 14 Å PNIPAM brush in 250 mM salt solutions as $+2$ °C and -6 °C in the presence of thiocyanate and acetate respectively.³⁶ These shifts are considerably smaller than the equivalent ± 10 °C shifts reported in Figure 8. Magnusson et al. reported that the salt response of POEGMA chains in solution is greater than PNIPAM.³⁵ They proposed that strong hydration of the hydrophilic side-chains would result in a greater response to Hofmeister anions. This may be sufficient to explain the enhanced shift to lower temperatures in potassium acetate solution. However, the larger polymer–aqueous solution interface introduced by the side chains would be expected to make the polymer more susceptible to an increase in interfacial tension at high chaotrope concentration that would result in a decrease in the LCST; an additional mechanism is therefore required to explain the impact of thiocyanate.³⁴ The magnitude of increase in the LCST by chaotropes is directly related to the number of accessible binding sites^{34, 60} and implies that there are more available in the reported PMEO₂MA brushes. The origin of this greater availability is unclear, but is possibly related to the comb architecture of the polymer chains. A systematic study of the temperature response of POEGMA copolymers with different side chain lengths or the use techniques sensitive to the binding of ions at interfaces such as vibrational sum frequency spectroscopy⁵⁹ would allow the enhanced specific ion response to be studied in more detail.

Conclusions

We have investigated the effect of salt concentration and identity on the temperature response of PMEO₂MA brushes using ellipsometry, NR and colloidal probe AFM measurements. The width (> 30 °C) and midpoint (21.2 ± 0.2 °C) of the temperature induced collapse transition in salt-free water of a PMEO₂MA brush with dry thickness 540 ± 30 Å is consistent with reported values.¹⁷ NR measurements showed a continuous transition between a collapsed, block-like structure at high temperatures to a single, swollen phase at low temperatures with no evidence of vertical phase separation, as previously observed for PNIPAM brushes.^{3, 51, 52} These structures are reflected in the transition from long to short range interactions in the AFM force curves with increasing temperature.

All three techniques show a large shift in the swelling transition of the brush to higher and lower temperatures with the addition of kosmotropic potassium acetate and chaotropic potassium thiocyanate respectively. The magnitude of this shift was greater than reported values for PNIPAM brushes of comparable thickness and grafting density,^{3, 36} with a five-fold increase in the observed response to 250 mM thiocyanate. This is consistent with behavior of free POEGMA chains in solution reported by Magnusson et al.³⁵ The MW of the brush was also found to affect the thermoresponse of the brush in potassium thiocyanate solution. A thicker brush showed no difference when increasing salt concentration from 250 to 500 mM, while thinner brushes continued to respond in this concentration range. This was attributed to a higher density of potential anion binding sites.^{34, 60}

Future experiments will investigate whether increasing the average length of PEG side chains results in further enhancement of the specific ion response as well as taking advantage of a recently developed neutron confinement cell for studying the structures formed by the brushes under mechanical confinement.⁶¹⁻⁶³ The large shift in temperature response at physiological concentrations of salts provides a pathway for modulating the thermoresponse in temperature sensitive applications.

Acknowledgements

This work was supported by an Australian Centre for Neutron Scattering Program Grant (PP4274).

TJM and BAH would like to thank AINSE Ltd for providing financial assistance (PGRA Awards). UNSW

Engineering is thanked for a Faculty Research Grant supporting SWP.

Supporting Material

Contains details of the brush synthesis, additional neutron reflectometry figures and tables, together with AFM experimental details and retraction force curves in the presence of specific ions.

References

1. Liu, R.; Fraylich, M.; Saunders, B. R. Thermoresponsive Copolymers: From Fundamental Studies to Applications. *Colloid and Polymer Science* **2009**, *287*, 627-643.
2. Schild, H. Poly(*N*-isopropylacrylamide): Experiment, Theory and Application. *Progress in Polymer Science* **1992**, *17*, 163-249.
3. Murdoch, T. J.; Humphreys, B. A.; Willott, J. D.; Gregory, K. P.; Prescott, S. W.; Nelson, A.; Wanless, E. J.; Webber, G. B. Specific Anion Effects on the Internal Structure of a Poly(*N*-isopropylacrylamide) Brush. *Macromolecules* **2016**, *49*, 6050-6060.
4. Lutz, J.-F.; Akdemir, Ö.; Hoth, A. Point by Point Comparison of two Thermosensitive Polymers Exhibiting a Similar LCST: Is the Age of Poly(NIPAM) Over? *Journal of the American Chemical Society* **2006**, *128*, 13046-13047.
5. Lutz, J. F. Polymerization of Oligo(ethylene glycol)(meth) acrylates: Toward New Generations of Smart Biocompatible Materials. *Journal of Polymer Science Part A: Polymer Chemistry* **2008**, *46*, 3459-3470.
6. Vancoillie, G.; Frank, D.; Hoogenboom, R. Thermoresponsive Poly(oligo ethylene glycol acrylates). *Progress in Polymer Science* **2014**, *39*, 1074-1095.
7. Vihola, H.; Laukkanen, A.; Valtola, L.; Tenhu, H.; Hirvonen, J. Cytotoxicity of Thermosensitive Polymers Poly(*N*-isopropylacrylamide), Poly(*N*-vinylcaprolactam) and Amphiphilically Modified Poly(*N*-vinylcaprolactam). *Biomaterials* **2005**, *26*, 3055-3064.
8. Kitano, H.; Kondo, T.; Suzuki, H.; Ohno, K. Temperature-Responsive Polymer-Brush Constructed on a Glass Substrate by Atom Transfer Radical Polymerization. *Journal of Colloid and Interface Science* **2010**, *345*, 325-331.
9. Anderson, C. R.; Abecunas, C.; Warrenner, M.; Laschewsky, A.; Wischerhoff, E. Effects of Methacrylate-Based Thermoresponsive Polymer Brush Composition on Fibroblast Adhesion and Morphology. *Cellular and Molecular Bioengineering* **2016**, DOI: 10.1007/s12195-016-0464-5, 1-14.
10. Sefcik, L. S.; Kaminski, A.; Ling, K.; Laschewsky, A.; Lutz, J.-F.; Wischerhoff, E. Effects of PEG-Based Thermoresponsive Polymer Brushes on Fibroblast Spreading and Gene Expression. *Cellular and Molecular Bioengineering* **2013**, *6*, 287-298.
11. Wischerhoff, E.; Uhlig, K.; Lankenau, A.; Börner, H. G.; Laschewsky, A.; Duschl, C.; Lutz, J. F. Controlled Cell Adhesion on PEG-Based Switchable Surfaces. *Angewandte Chemie International Edition* **2008**, *47*, 5666-5668.
12. de Vos, W. M.; Leermakers, F. A.; Lindhoud, S.; Prescott, S. W. Modeling the Structure and Antifouling Properties of a Polymer Brush of Grafted Comb-Polymers. *Macromolecules* **2011**, *44*, 2334-2342.

13. Gao, X.; Kucerka, N.; Nieh, M.-P.; Katsaras, J.; Zhu, S.; Brash, J. L.; Sheardown, H. Chain Conformation of a New Class of PEG-Based Thermoresponsive Polymer Brushes Grafted on Silicon as Determined by Neutron Reflectometry. *Langmuir* **2009**, *25*, 10271-10278.
14. Teixeira, F.; Popa, A. M.; Guimond, S.; Hegemann, D.; Rossi, R. M. Synthesis of Poly(oligo (ethylene glycol) methacrylate)-Functionalized Membranes for Thermally Controlled Drug Delivery. *Journal of Applied Polymer Science* **2013**, *129*, 636-643.
15. Tan, I.; Zarafshani, Z.; Lutz, J.-F.; Titirici, M.-M. PEGylated Chromatography: Efficient Bioseparation on Silica Monoliths Grafted with Smart Biocompatible Polymers. *ACS Applied Materials & Interfaces* **2009**, *1*, 1869-1872.
16. Zhuang, P.; Dirani, A.; Glinel, K.; Jonas, A. M. Temperature Dependence of the Surface and Volume Hydrophilicity of Hydrophilic Polymer Brushes. *Langmuir* **2016**, *32*, 3433-3444.
17. Laloyaux, X.; Mathy, B.; Nysten, B.; Jonas, A. Surface and Bulk Collapse Transitions of Thermoresponsive Polymer Brushes. *Langmuir* **2010**, *26*, 838-847.
18. Jonas, A.; Glinel, K.; Oren, R.; Nysten, B.; Huck, W. T. S. Thermo-Responsive Polymer Brushes with Tunable Collapse Temperatures in the Physiological Range. *Macromolecules* **2007**, *40*, 4403-4405.
19. Svetushkina, E.; Pureskiy, N.; Ionov, L.; Stamm, M.; Synytska, A. A Comparative Study on Switchable Adhesion between Thermoresponsive Polymer Brushes on Flat and Rough Surfaces. *Soft Matter* **2011**, *7*, 5691-5696.
20. Kessel, S.; Schmidt, S.; Müller, R.; Wischerhoff, E.; Laschewsky, A.; Lutz, J. F.; Uhlig, K.; Lankenau, A.; Duschl, C.; Fery, A. Thermoresponsive PEG-based Polymer Layers: Surface Characterization with AFM Force Measurements. *Langmuir* **2009**, *26*, 3462-3467.
21. Synytska, A.; Svetushkina, E.; Pureskiy, N.; Stoychev, G.; Berger, S.; Ionov, L.; Bellmann, C.; Eichhorn, K.-J.; Stamm, M. Biocompatible Polymeric Materials with Switchable Adhesion Properties. *Soft Matter* **2010**, *6*, 5907-5914.
22. Baulin, V. A.; Halperin, A. Signatures of a Concentration-Dependent Flory χ Parameter: Swelling and Collapse of Coils and Brushes. *Macromolecular Theory and Simulations* **2003**, *12*, 549-559.
23. Halperin, A.; Kroger, M. Collapse of Thermoresponsive Brushes and the Tuning of Protein Adsorption. *Macromolecules* **2011**, *44*, 6986-7005.
24. Sun, S.; Wu, P. On the Thermally Reversible Dynamic Hydration Behavior of Oligo(ethylene glycol) methacrylate-based Polymers in Water. *Macromolecules* **2012**, *46*, 236-246.
25. Lo Nostro, P.; Ninham, B. W. Hofmeister Phenomena: An Update on Ion Specificity in Biology. *Chemical Reviews* **2012**, *112*, 2286-2322.
26. Hofmeister, F. On the understanding of the effects of salts. *Arch. Exp. Pathol. Pharmacol. (Leipzig)* **1888**, *24*, 247-260.
27. Swann, J. M. G.; Bras, W.; Topham, P. D.; Howse, J. R.; Ryan, A. Effect of the Hofmeister Anions upon the Swelling of a Self-Assembled pH-Responsive Hydrogel. *Langmuir* **2010**, *26*, 10191-10197.
28. Azzaroni, O.; Moya, S.; Farhan, T.; Brown, A. A.; Huck, W. T. Switching the Properties of Polyelectrolyte Brushes via "Hydrophobic Collapse". *Macromolecules* **2005**, *38*, 10192-10199.
29. Kou, R.; Zhang, J.; Wang, T.; Liu, G. Interactions between Polyelectrolyte Brushes and Hofmeister Ions: Chaotropes versus Kosmotropes. *Langmuir* **2015**, *31*, 10461-10468.
30. Willott, J. D.; Murdoch, T. J.; Humphreys, B. A.; Edmondson, S.; Wanless, E. J.; Webber, G. B. Anion-specific Effects on the Behavior of pH-Sensitive Polybasic Brushes. *Langmuir* **2015**, *31*, 3707-3717.
31. Willott, J. D.; Murdoch, T. J.; Webber, G. B.; Wanless, E. J. Nature of the Specific Anion Response of a Hydrophobic Weak Polyelectrolyte Brush Revealed by AFM Force Measurements. *Macromolecules* **2016**, *49*, 2327-2338.
32. Henry, C. L.; Craig, V. S. J. The Link between Ion Specific Bubble Coalescence and Hofmeister Effects Is the Partitioning of Ions within the Interface. *Langmuir* **2010**, *26*, 6478-6483.

33. López-León, T.; Ortega-Vinuesa, J. L.; Bastos-González, D. Ion-Specific Aggregation of Hydrophobic Particles. *ChemPhysChem* **2012**, *13*, 2382-2391.
34. Zhang, Y.; Cremer, P. S. Chemistry of Hofmeister Anions and Osmolytes. *Annual Review of Physical Chemistry* **2010**, *61*, 63-83.
35. Magnusson, J. P.; Khan, A.; Pasparakis, G.; Saeed, A. O.; Wang, W.; Alexander, C. Ion-Sensitive “Isothermal” Responsive Polymers Prepared in Water. *Journal of the American Chemical Society* **2008**, *130*, 10852-10853.
36. Humphreys, B. A.; Willott, J. D.; Murdoch, T. J.; Webber, G. B.; Wanless, E. J. Specific Ion Modulated Thermoresponse of Poly(*N*-isopropylacrylamide) Brushes. *Physical Chemistry Chemical Physics* **2016**, *18*, 6037-6046.
37. Yamamoto, S.-i.; Pietrasik, J.; Matyjaszewski, K. Temperature-and pH-responsive dense copolymer brushes prepared by ATRP. *Macromolecules* **2008**, *41*, 7013-7020.
38. Lutz, J.-F.; Hoth, A.; Schade, K. Design of Oligo(ethylene glycol)-Based Thermo-responsive Polymers: An Optimization Study. *Designed Monomers and Polymers* **2009**, *12*, 343-353.
39. Matyjaszewski, K.; Dong, H.; Jakubowski, W.; Pietrasik, J.; Kusumo, A. Grafting from surfaces for “everyone”: ARGET ATRP in the presence of air. *Langmuir* **2007**, *23*, 4528-4531.
40. Nelson, A. Co-Refinement of Multiple-Contrast Neutron/X-Ray Reflectivity Data using MOTOFIT. *Journal of Applied Crystallography* **2006**, *39*, 273-276.
41. James, M.; Nelson, A.; Holt, S. A.; Saerbeck, T.; Hamilton, W. A.; Klose, F. The Multipurpose Time-of-Flight Neutron Reflectometer “Platypus” at Australia's OPAL Reactor. *Nuclear Instruments and Methods in Physics Research Section A: Accelerators, Spectrometers, Detectors and Associated Equipment* **2011**, *632*, 112-123.
42. Murdoch, T. J.; Humphreys, B. A.; Willott, J. D.; Gregory, K. P.; Prescott, S. W.; Nelson, A.; Wanless, E. J.; Webber, G. B. Specific Anion Effects on the Internal Structure of a poly(*N*-isopropylacrylamide) Brush. *Macromolecules* **2016**, submitted.
43. Sudre, G.; Hourdet, D.; Creton, C.; Cousin, F.; Tran, Y. pH-Responsive Swelling of Poly(acrylic acid) Brushes Synthesized by the Grafting Onto Route. *Macromolecular Chemistry and Physics* **2013**, *214*, 2882-2890.
44. Habicht, J.; Schmidt, M.; Rühle, J.; Johannsmann, D. Swelling of Thick Polymer Brushes Investigated with Ellipsometry. *Langmuir* **1999**, *15*, 2460-2465.
45. Zhulina, E.; Borisov, O.; Pryamitsyn, V.; Birshtein, T. Coil-Globule Type Transitions in Polymers. 1. Collapse of Layers of Grafted Polymer Chains. *Macromolecules* **1991**, *24*, 140-149.
46. Dunlop, I. E.; Thomas, R. K.; Titmus, S.; Osborne, V.; Edmondson, S.; Huck, W. T.; Klein, J. Structure and Collapse of a Surface-Grown Strong Polyelectrolyte Brush on Sapphire. *Langmuir* **2012**, *28*, 3187-3193.
47. Jia, H.; Wildes, A.; Titmuss, S. Structure of pH-Responsive Polymer Brushes Grown at the Gold–Water Interface: Dependence on Grafting Density and Temperature. *Macromolecules* **2011**, *45*, 305-312.
48. Kobayashi, M.; Ishihara, K.; Takahara, A. Neutron Reflectivity Study of the Swollen Structure of Polyzwitterion and Polyelectrolyte Brushes in Aqueous Solution. *Journal of Biomaterials Science, Polymer Edition* **2014**, *25*, 1673-1686.
49. Moglianetti, M.; Webster, J. R.; Edmondson, S.; Armes, S. P.; Titmuss, S. Neutron Reflectivity Study of the Structure of pH-Responsive Polymer Brushes Grown from a Macroinitiator at the Sapphire–Water Interface. *Langmuir* **2010**, *26*, 12684-12689.
50. Martinez, A. P.; Carrillo, J.-M. Y.; Dobrynin, A. V.; Adamson, D. H. Distribution of Chains in Polymer Brushes Produced by a “Grafting From” Mechanism. *Macromolecules* **2016**, *49*, 547-553.
51. Elliott, L. C.; Jing, B.; Akgun, B.; Zhu, Y.; Bohn, P. W.; Fullerton-Shirey, S. K. Loading and Distribution of a Model Small Molecule Drug in Poly(*N*-isopropylacrylamide) Brushes: A Neutron Reflectometry and AFM Study. *Langmuir* **2013**, *29*, 3259-3268.

52. Yim, H.; Kent, M.; Satija, S.; Mendez, S.; Balamurugan, S.; Balamurugan, S.; Lopez, G. Evidence for Vertical Phase Separation in Densely Grafted, High-Molecular-Weight Poly(*N*-isopropylacrylamide) Brushes in Water. *Physical Review E* **2005**, *72*, 051801.
53. Goodman, D.; Kizhakkedathu, J. N.; Brooks, D. E. Attractive Bridging Interactions in Dense Polymer Brushes in Good Solvent Measured by Atomic Force Microscopy. *Langmuir* **2004**, *20*, 2333-2340.
54. Wang, R. L. C.; Kreuzer, H. J.; Grunze, M. Molecular Conformation and Solvation of Oligo(ethylene glycol)-Terminated Self-Assembled Monolayers and Their Resistance to Protein Adsorption. *The Journal of Physical Chemistry B* **1997**, *101*, 9767-9773.
55. Yu, Y.; Kieviet, B. D.; Liu, F.; Siretanu, I.; Kutnyanszky, E.; Vancso, G. J.; de Beer, S. Stretching of Collapsed Polymers causes an Enhanced Dissipative Response of PNIPAM Brushes Near their LCST. *Soft Matter* **2015**, *11*, 8508-8516.
56. Varma, S.; Bureau, L.; Débarre, D. The Conformation of Thermoresponsive Polymer Brushes Probed by Optical Reflectivity. *Langmuir* **2016**, *32*, 3152-3163.
57. Horinek, D.; Netz, R. R. Specific Ion Adsorption at Hydrophobic Solid Surfaces. *Phys. Rev. Lett.* **2007**, *99*, 226104.
58. Rembert, K. B.; Paterová, J.; Heyda, J.; Hilty, C.; Jungwirth, P.; Cremer, P. S. Molecular Mechanisms of Ion-Specific Effects on Proteins. *Journal of the American Chemical Society* **2012**, *134*, 10039-10046.
59. Chen, X.; Yang, T.; Kataoka, S.; Cremer, P. S. Specific Ion Effects on Interfacial Water Structure Near Macromolecules. *Journal of the American Chemical Society* **2007**, *129*, 12272-12279.
60. Zhang, Y.; Furyk, S.; Sagle, L. B.; Cho, Y.; Bergbreiter, D. E.; Cremer, P. S. Effects of Hofmeister Anions on the LCST of PNIPAM as a Function of Molecular Weight. *The Journal of Physical Chemistry B* **2007**, *111*, 8916-8924.
61. Abbott, S. B.; de Vos, W. M.; Mears, L. L.; Cattoz, B.; Skoda, M. W.; Barker, R.; Richardson, R. M.; Prescott, S. W. Is Osmotic Pressure Relevant in the Mechanical Confinement of a Polymer Brush? *Macromolecules* **2015**, *48*, 2224-2234.
62. Abbott, S. B.; de Vos, W. M.; Mears, L. L. E.; Skoda, M.; Dalglish, R.; Edmondson, S.; Richardson, R. M.; Prescott, S. W. Switching the Interpenetration of Confined Asymmetric Polymer Brushes. *Macromolecules* **2016**, *49*, 4349-4357.
63. Wei, Z.; Prescott, S. W. Scattering Approaches to Probing Surface Layers Under Confinement. *Current Opinion in Colloid & Interface Science* **2015**, *20*, 253-260.

Supporting Material

Enhanced Specific Ion Effects in Ethylene Glycol-based Thermoresponsive Polymer Brushes

Timothy J. Murdoch,^a Ben A. Humphreys,^a Joshua D. Willott,^a Stuart W. Prescott,^b Andrew Nelson,^c
Grant B. Webber^a, Erica J. Wanless,^{a*}

^a Priority Research Centre for Advanced Particle Processing and Transport, University of Newcastle,
Callaghan, NSW 2308, Australia

^b School of Chemical Engineering, UNSW Australia, UNSW Sydney, NSW 2052, Australia

^c Australian Nuclear Science and Technology Organisation, Lucas Heights, NSW 2234, Australia

*Corresponding author Erica J. Wanless, email: erica.wanless@newcastle.edu.au, phone: +61 2 4033
9355

PMEO₂MA Brush Synthesis Details

Functionalized wafers were placed in 30 mL glass vials and deoxygenated for 15 min under vented N₂ flow. CuBr₂, ligand (bipy or HMTETA), MEO₂MA monomer and solvent were combined in a round bottomed flask and deoxygenated while stirring for 15 min. The sodium ascorbate was then added and the solution deoxygenated for a further 15 min over which time the solution changed color from a transparent blue/green to transparent dark brown. 10 mL of the polymerization solution (enough to submerge the functionalized wafers) was then syringed into the reaction vials to initiate the brush polymerization. This was carried out under slight positive N₂ pressure at ambient temperature (22±0.5 °C). When the target polymerization time was reached the wafers were removed from the reaction vial and rinsed with ethanol followed by copious water then dried under a stream of N₂. This procedure was up-scaled for the 100 mm neutron reflectometry silicon wafer. Typical growth kinetics for the two recipes are given in Figure S1. Both recipes produce controlled growth for synthesis times ≤ 2 h as evidenced by the approximately linear increase in brush thickness.¹ Different growth kinetics allow better targeting of optimum brush thicknesses for the various characterization techniques. The faster growth in the HMTETA recipe is a result of HMTETA being a more active ATRP ligand than bipy.²

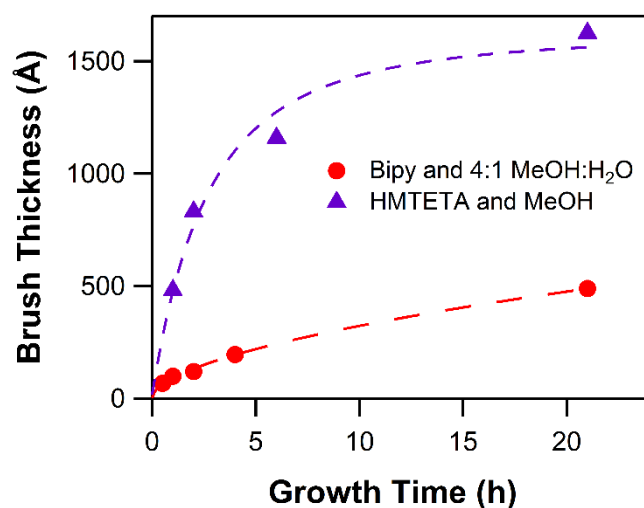


Figure S1: Polymerization kinetics of PMEO₂MA brushes as a function of ligand. Lines are given to guide the eye.

Additional Neutron Reflectometry Tables and Figures

Tables S1–4 present the parameters for the model volume fraction profiles for each salt type. The silicon dioxide layer used for all fits was 16 Å with a 3 Å roughness to the silicon substrate. An SLD of $3.83 \times 10^{-6} \text{ \AA}^{-2}$ was determined for the native oxide layer in D₂O solutions (based on 13.5% solvent penetration, see Figure S2).

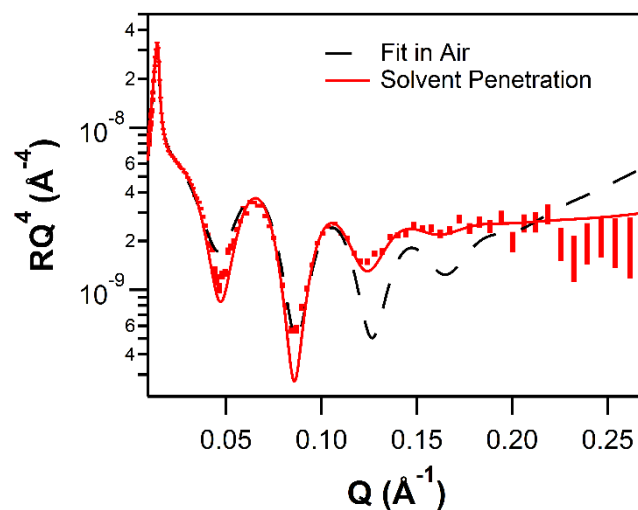


Figure S2. Comparison of fits of neutron reflectometry data with and without solvent penetration in native oxide correction. Data corresponds to for a $140 \pm 10 \text{ \AA}$ PMEO₂MA brush in D₂O at 45 °C.

Table S1. Tabulated data for D₂O model parameters

Temperature (°C)	45	40	35	30	25	20	15
χ^2	6	7	10	3	2	3	4
Number Interior Layers	1	1	1	2	3	3	3
Int. Thick. 1 (Å) ^a	154.4	156.7	161.8	20.5	19.5	20.2	19.2
ϕ_1	0.90	0.89	0.86	0.93	1.00	0.98	0.93
Rough. 1 ^b	2.0	2.0	2.0	2.0	2.0	2.0	2.0
Int. Thick. 2 (Å)				144.2	147.6	196.9	262.6
ϕ_2				0.80	0.65	0.45	0.35
Rough. 2 ^c				6.2	13.0	13.1	10.5
Int. Thick. 3 (Å)					33.4	80.2	199.1
ϕ_3					0.52	0.28	0.10
Rough. 3					15.0	38.0	91.0
Rough. Ext. Solv. (Å) ^d	15.8	16.5	18.6	22.5	29.8	69.8	100.0

^aInterior layer thickness, ^bInterior roughness with previous layer, ^cFits are largely insensitive to this parameter, ^dRoughness between exterior and solvent

Table S2. Tabulated data for 250 mM potassium acetate model parameters

Temperature (°C)	40	35	30	25	20	15
χ^2	5	5	6	4	3	4
Number Interior Layers	1	1	1	2	2	2
Int. Thick. 1 (Å) ^a	149.2	151.2	154.2	19.0	21.4	20.2
ϕ_1	0.90	0.89	0.87	0.90	0.90	1.00
Rough. 1 ^b	2.0	2.0	2.0	2.0	2.0	2.0
Int. Thick. 2 (Å)				138.0	152.3	198.4
ϕ_2				0.82	0.72	0.55
Rough. 2 ^c				1.0	6.4	10.3
Int. Thick. 3 (Å)						
ϕ_3						
Rough. 3						
Rough. Ext. Solv. (Å) ^d	15.9	16.7	18.2	20.3	25.1	40.4

^aInterior layer thickness, ^bInterior roughness with previous layer, ^cFits are largely insensitive to this parameter, ^dRoughness between exterior and solvent

Table S3. Tabulated data for 250 mM potassium thiocyanate model parameters

Temperature (°C)	45	40	35	30	25	20	15
χ^2	5	4	2	2	2	3	4
Number Interior Layers	1	2	2	3	3	1	1
Int. Thick. 1 (Å) ^a	150.0	20.6	22.1	22.7	20.2	18.7	16.9
ϕ_1	0.88	0.91	1.00	1.00	1.00	0.98	0.98
Rough. 1 ^b	2.0	2.0	2.0	2.0	2.0	2.0	2.0
Int. Thick. 2 (Å)		133.6	166.5	237.2	288.2	41.5	41.5
ϕ_2		0.85	0.66	0.37	0.29	0.19	0.19
Rough. 2 ^c		1.0	15.2	9.7	9.2	4.6	4.6
Int. Thick. 3 (Å)				195.8	242.6	244.6	244.6
ϕ_3				0.14	0.10	0.51	0.51
Rough. 3				87.9	97.9	35.5	35.5
ϕ_0						0.26	0.23
Characteristic H (Å) ^d						475.2	574.3
Rough. Int. Ext. (Å) ^e						7.6	7.0
Rough. Ext. Solv. (Å) ^f	19.5	23.0	37.1	99.9	100.0	5.0	5.0

^aInterior layer thickness, ^bInterior roughness with previous layer, ^cFits are largely insensitive to this parameter, ^dcharacteristic height of tail, ^eRoughness between interior and exterior, ^fRoughness between exterior and solvent

Table S4. Tabulated data for 500 mM potassium thiocyanate model parameters

Temperature (°C)	45	40	35	30	25	20	15
χ^2	3	2	3	3	3	5	3
Number Interior Layers	2	2	3	3	1	1	1
Int. Thick. 1 (Å) ^a	21.6	22.3	22.3	20.1	18.6	16.7	15.6
ϕ_1	0.91	1.00	1.00	1.00	0.96	0.96	0.95
Rough. 1 ^b	2.0	2.0	2.0	2.0	2.0	2.0	2.0
Int. Thick. 2 (Å)	130.3	157.9	217.5				
ϕ_2	0.85	0.69	0.39				
Rough. 2 ^c	1.1	13.1	10.3				
Int. Thick. 3 (Å)			141.4				
ϕ_3			0.24				
Rough. 3			66.9				
ϕ_0					0.3	0.2	0.2
Characteristic H (Å) ^d					503.0	622.0	668.9
Rough. Int. Ext. (Å) ^e					7.6	6.9	6.6
Rough. Ext. Solv. (Å) ^f	22.2	34.6	99.6	100.0	5.0	5.0	5.0

^aInterior layer thickness, ^bInterior roughness with previous layer, ^cFits are largely insensitive to this parameter, ^dcharacteristic height of tail, ^eRoughness between interior and exterior, ^fRoughness between exterior and solvent

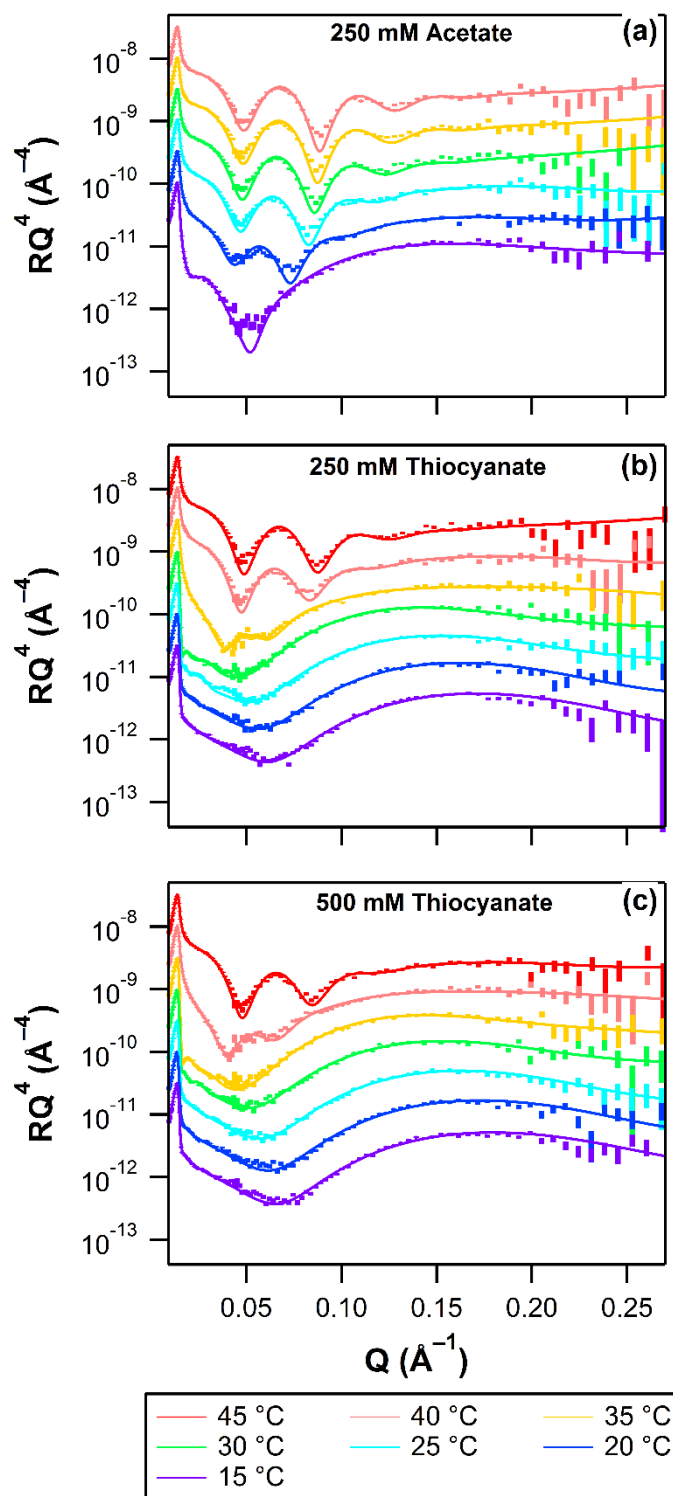


Figure S3. Reflectivity data as a function of temperature for a $140 \pm 10 \text{ \AA}$ PMEO₂MA brush immersed in (a) 250 mM potassium acetate, (b) 250 mM thiocyanate, and (c) 500 mM thiocyanate D₂O solutions. Data is offset for clarity with the respective profile recorded at 45 °C plotted using measured data.

Atomic Force Microscopy experimental details

Single-molecule force spectroscopy measurements (SMFS) were performed using a silicon nitride cantilever with backside reflective gold coating (DNP-10, Bruker, USA). For the colloid probe studies a single, dry native silica microsphere (Bangs Laboratories Inc., USA, diameter $\sim 15 \mu\text{m}$) was glued (using two-part epoxy resin) onto a tipless rectangular silicon nitride cantilever with an aluminium backside coating (HQ:NSC36/tipless/Al BS, Mikromasch, USA). The spring constant (k_N) of the cantilevers used was measured using the built-in thermal noise method (an average of 5 discrete measurements). For the SMFS measurements two different cantilevers were used $k_N = 0.1$ and $0.6 \text{ N}\cdot\text{m}^{-2}$, and for the colloid probe study $k_N = 1.0 \text{ N}\cdot\text{m}^{-2}$ (measured before and after gluing of colloid probe). Prior to in situ measurements, the fluid cell, O-ring and cantilevers were cleaned via ethanol and water rinses. The cantilevers were then exposed to UV/O₃ (15 min for SMFS cantilever and 2 min for colloid probe cantilever).

For both the SMFS and colloid probe studies the PMEO₂MA brush was first exposed to H₂O at 22 °C. Upon completion of each solution condition, 10 – 20 mL of the next solution was flowed through the fluid cell, after which the brush was allowed to equilibrate for at least 20 min. Our studies revealed that this equilibration time was sufficient, with no drift observed in the measured force curves over time. Cantilever deflection vs displacement data were converted to normal force vs apparent separation curves using standard methods as outlined by Ralston et al.³

All SMFS experiments were performed in pure water at $<20 \text{ }^\circ\text{C}$; an environment where the ellipsometry data in Figure 2 shows that PMEO₂MA brushes are fully swollen. Consequently, these conditions provided the best opportunity to adhere and stretch individual chains which this analysis requires. The SMFS methodology and data analysis is explained in detail elsewhere.⁴

The colloid probe force measurements were performed over approximately 60 hours with the PMEO₂MA brush immersed in solution throughout. All force curves were collected using a piezo ramp size of $1.5 \mu\text{m}$, a tip velocity of $0.3 \mu\text{m}\cdot\text{s}^{-1}$ during both approach and retraction, no surface dwell and at constant maximum indentation load. Force measurements were performed in pure water and in the presence of aqueous 250 mM potassium acetate and 250 mM potassium thiocyanate electrolyte at four different temperatures: 10, 20.5, 30 and 40 °C. The solution pH was maintained at 5.5 ± 0.1 . A total of 25 curves were collected at each condition. Average approach and retraction curves were determined using a custom MATLAB script as described elsewhere and were used to select the most representative curve for presentation.⁴

AFM Retraction Curves

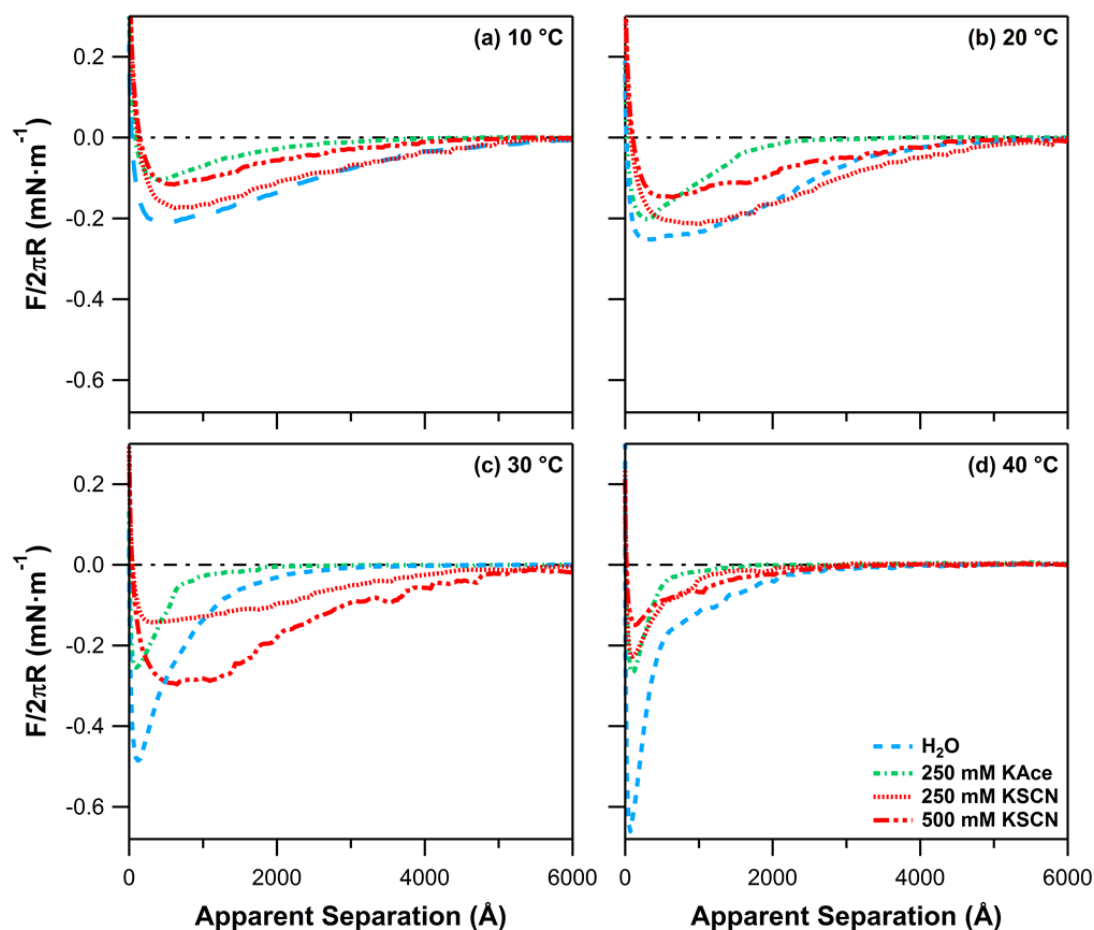


Figure S4. Force versus apparent separation curves for the retraction of a silica colloid probe away from a $215 \pm 10 \text{ \AA}$ PMEO₂MA brush in pure H₂O, 250 mM potassium acetate, 250 mM potassium thiocyanate and 500 mM potassium thiocyanate.

References for Supporting Material

1. Kim, J. B.; Huang, W.; Miller, M. D.; Baker, G. L.; Bruening, M. L. Kinetics of Surface-Initiated Atom Transfer Radical Polymerization. *Journal of Polymer Science Part A: Polymer Chemistry* **2003**, *41*, 386-394.
2. Matyjaszewski, K.; Tsarevsky, N. V. Macromolecular engineering by atom transfer radical polymerization. *Journal of the American Chemical Society* **2014**, *136*, 6513-6533.
3. Ralston, J.; Larson, I.; Rutland, M. W.; Feiler, A. A.; Kleijn, M. Atomic Force Microscopy and Direct Surface Force Measurements (IUPAC Technical Report). *Pure and Applied Chemistry* **2005**, *77*, 2149-2170
4. Willott, J. D.; Murdoch, T. J.; Webber, G. B.; Wanless, E. J. Nature of the Specific Anion Response of a Hydrophobic Weak Polyelectrolyte Brush Revealed by AFM Force Measurements. *Macromolecules* **2016**, *49*, 2327-2338.